Nuclear Engineering and Technology 53 (2021) 2556–2563

Contents lists available at ScienceDirect

Nuclear Engineering and Technology

journal homepage: www.elsevier.com/locate/net

Original Article

Control of a pressurized light-water nuclear reactor two-point kinetics model with the performance index-oriented PSO

Seyed Mohammad Hossein Mousakazemi

Department of Physics, Faculty of Basic Sciences, Payame Noor University, 19395-4697 Tehran, Iran

ARTICLE INFO

Article history:
Received 4 May 2020
Received in revised form
29 January 2021
Accepted 16 February 2021
Available online 9 March 2021

Keywords:
Pressurized light-water reactor two-point kinetics model
Integral of the absolute error (IAE)
Integral of square error (ISE)
Integral of time-absolute error (ITAE)
Integral of time-square error (ITSE)
Proportional–integral–derivative (PID) controller

ABSTRACT

Metaheuristic algorithms can work well in solving or optimizing problems, especially those that require approximation or do not have a good analytical solution. Particle swarm optimization (PSO) is one of these algorithms. The response quality of these algorithms depends on the objective function and its regulated parameters. The nonlinear nature of the pressurized light-water nuclear reactor (PWR) dynamics is a significant target for PSO. The two-point kinetics model of this type of reactor is used because of fission products properties. The proportional–integral–derivative (PID) controller is intended to control the power level of the PWR at a short-time transient. The absolute error (IAE), integral of square error (ISE), integral of time-absolute error (ITAE), and integral of time-square error (ITSE) objective functions have been used as performance indexes to tune the PID gains with PSO. The optimization results with each of them are evaluated with the number of function evaluations (NFE). All performance indexes achieve good results with differences in the rate of over/under-shoot or convergence rate of the cost function, in the desired time domain.

1. Introduction

A performance index has an important role in the performance and speed of the metaheuristic algorithms. One of these algorithms is particle swarm optimization (PSO). This algorithm has shown its optimizing performance in many problems, especially those that do not have a clear analytical solution or are difficult to solve. The nuclear reactor dynamics is nonlinear such as a pressurized water reactor (PWR), which can be solved analytically by linearizing the state-space equations. One of the most effective controllers for this reactor type is proportional–integral–derivative (PID), and one of the methods for tuning its gains is PSO. This algorithm has been used frequently in various nuclear industry issues. Câmara Augusto et al. [1] used PSO for a nuclear reactor reload issue. In their work, a new method was proposed to communicate between particles in PSO. Wang et al. [2] were used PSO to optimize the parameter of an AP1000 reactor. In PSO, the control parameter as an objective function was directly incorporated in the simulation results. PSO was used for a power ascension path of a boiling water reactor [3]. In their work, the control rod movement was searched as an objective function. The fuel loading pattern of a swimming pool type material test reactor was optimized with PSO as maximizing the effective multiplication factor constrained to decrease the power peaking factor [4]. Wang et al. [5] used a hybrid fault diagnosis methodology with PSO for the safety and public health of a nuclear power plant (NPP). Recently, PSO has been used for molten salt breeder reactor power control with internal model control PID [6].

In a PWR nuclear reactor, axial xenon oscillation leads to axial offset (AO) power-distribution. Therefore, it is better to use a multi-point kinetics model. These models also have better accuracy than the point-kinetics model. In this work, the conventional two-point kinetics reactor model of a typical PWR is used. The power level of this model is controlled with two PSO-tuned PID controller. PSO as a metaheuristic algorithm and its optimizing case (PIDs) depend on the defined objective function as the performance index. Common integrals of the error function are used to tune the PID gains, i.e. integral of the absolute error (IAE), integral of square error (ISE), integral of time-absolute error (ITAE), and integral of time-square error (ITSE). The central processing unit (CPU) time criterion is commonly used to compare two algorithms. Recently, Mousakazemi [7] has been proposed the number of function evaluations (NFE) instead of the CPU time method. These performance indexes are compared based on the NFE and quality of the closed-loop PID controlling system.

E-mail addresses: smh_mousakazemi@pnu.ac.ir, mousakazemi@gmail.com.

https://doi.org/10.1016/j.net.2021.02.018

Nomenclature

n	neutron density, cm^{-3}
n_0	initial neutron density in an equilibrium state, cm^{-3}
n_r	neutron density relative to initial density, $n/\ n_0$
c	precursor densitycm^{-3}
c_0	initial precursor density in an equilibrium statecm^{-3}
c_r	precursor density relative to initial density, $c/\ c_0$
w_{11}	coupling coefficient of node 1 to itself
w_{12}	coupling coefficient between nodes 1 and 2
w_{22}	coupling coefficient of node 2 to itself
w_{21}	coupling coefficient between nodes 2 and 1
D	diffusion coefficient, cm
v	thermal neutron speed, cm/s
ΔH	axial height of each core half, cm
d	axial distance between the two nodes center, cm
$n(0)$	steady-state value of neutron density at initial rated power, cm^{-3}
Xe	xenon density, cm^{-3}
$Xe0$	initial value of j-th node xenon density, cm^{-3}
I	Iodine density of node j, cm^{-3}
T_f	average temperature of the fuel, $^\circ C$
$T0$	initial value of fuel temperature, $^\circ C$
T_c	average temperature of coolant ($T_c = (T_e + T_l)/\ 2$), $^\circ C$
$T0_c$	initial value of coolant temperature, $^\circ C$
T_e	inlet temperature of the coolant, $^\circ C$
T_l	outlet temperature of the coolant, $^\circ C$
ρ	total reactivity, δK/K
$\delta\rho_r$	induced reactivity due to control rod movement, δK/K
Z_r	control rod speed, fraction of corelength/s
G_r	total reactivity of control rod, δK/K
β_i	i-th group effective delayed neutron fraction
β	effective delayed-neutron fraction, $\beta = \sum_{i=1}^{3} \beta_i$
l	generation time of neutron, s
λ_i	decay constant of i-th delayed-neutron group, s^{-1}
γ_{Xe}	xenon yield per fission
λ_{Xe}	decay constant of xenon, s^{-1}
γ_I	Iodine yield per fission
λ_I	decay constant of Iodine, s^{-1}
Σ_f	macroscopic fission cross-section of the thermal neutron, cm^{-1}
σ_{Xe}	microscopic thermal neutron absorption cross-section of xenon, cm^2
G	useful thermal energy liberated per fission of ^{235}U, MW·s
V	volume of each core half, cm^3
f_f	fraction of deposited power in fuel
μ_f	total heat capacity of fuel, MW/$^\circ C$
μ_c	total heat capacity of coolant, MW·s/$^\circ C$
M	mass flow rate time heat capacity of water, MW/$^\circ C$
Ω	coefficient of heat transfer between fuel and coolant MW/$^\circ C$
α_f	fuel temperature coefficient, $(\delta K/K)/^\circ C$
α_c	coolant temperature coefficient, $(\delta K/K)/^\circ C$
P_0	rated power, MW
j	node number $= 1, 2$
K_P	proportional gain, $\in \mathbb{R}$
K_I	integral gain, $\in \mathbb{R}$
K_D	derivative gain, $\in \mathbb{R}$
$u(t)$	$= Z_r$
$e(t)$	tracking error between output and set-point

2. Materials and methods

2.1. Reactor model

The 16th order model is used in this paper. The two-point kinetics reactor model is considered in the neutronic equations, based on the three groups of the delayed-neutron precursors. In this paper, the core is axially divided into two halves (nodes), respectively, for the lower and upper half. Also, each node is affected by the other because of neutron diffusion [8,9].

$$\begin{cases} \dfrac{dn_{r_1}}{dt} = \dfrac{\rho_1 - \beta}{l_1} n_{r1} + \sum_{i=1}^{3} \dfrac{\beta_i}{l_1} c_{r1,i} - w_{11} n_{r1} + w_{12} n_{r2} \\ \dfrac{dC_{r1,i}}{dt} = \lambda_i n_{r1} - \lambda_i c_{r1,i} \quad (i = 1,2,3) \end{cases} \tag{1}$$

$$\begin{cases} \dfrac{dn_{r2}}{dt} = \dfrac{\rho_2 - \beta}{l_2} n_{r2} + \sum_{i=1}^{3} \dfrac{\beta_i}{l_2} c_{r2,i} - w_{22} n_{r2} + w_{21} n_{r1} \\ \dfrac{dC_{r2,i}}{dt} = \lambda_i n_{r2} - \lambda_i c_{r2,i} \quad (i = 1,2,3) \end{cases} \tag{2}$$

$$w_{11} = \frac{D_1 v}{\Delta H_1 d_{21}},\ w_{12} = \frac{D_1 v}{\Delta H_1 d_{21}} \frac{n_2(0)}{n_1(0)},\ w_{22} = \frac{D_2 v}{\Delta H_2 d_{12}},\ w_{21} = \frac{D_2 v}{\Delta H_2 d_{12}} \frac{n_1(0)}{n_2(0)} \tag{3}$$

The core reactivity is influenced by several factors in a PWR: neutron poisons feedback; especially xenon, feedback of the fuel and coolant temperatures, and injection reactivity caused by control rods movement. In this paper, fuel and coolant temperature equations are based on the lumped model. Also, two control rod banks are considered, which individually affect each half of the core.

$$\begin{cases} \dfrac{dXe_j}{dt} = \left(\gamma_{Xe}\Sigma_{f_j} - \sigma_a^{Xe_j} Xe_j\right) \dfrac{P_0}{G\Sigma_{f_j} V_j} n_{r_j} - \lambda_{Xe} Xe_j + \lambda_I I_j \\ \dfrac{dI_j}{dt} = \gamma_I \Sigma_{f_j} \dfrac{P_0}{G\Sigma_{f_j} V_j} n_{r_j} - \lambda_I I_j \end{cases} \tag{4}$$

$$\frac{dT_f}{dt} = \frac{f_f P_0}{\mu_f} n_r - \frac{\Omega}{\mu_f} T_f + \frac{\Omega}{2\mu_f}(T_e + T_l) \tag{5}$$

$$\frac{dT_l}{dt} = \frac{\left(1 - f_f\right) P_0}{\mu_c} n_r + \frac{\Omega}{\mu_c} T_f + \frac{M}{\mu_c}(T_e - T_l) - \frac{\Omega}{2\mu_c}(T_e + T_l) \tag{6}$$

$$\frac{d\rho_{r_j}}{dt} = G_{r_j} Z_{r_j} \tag{7}$$

$$\rho_j = \delta\rho_{r_j} + \alpha_f\left(T_f - T0_f\right) + \alpha_c(T_c - T0_c) - \frac{\sigma_{Xe_j}}{\Sigma_{f_j}}\left(Xe_j - Xe0_j\right) \tag{8}$$

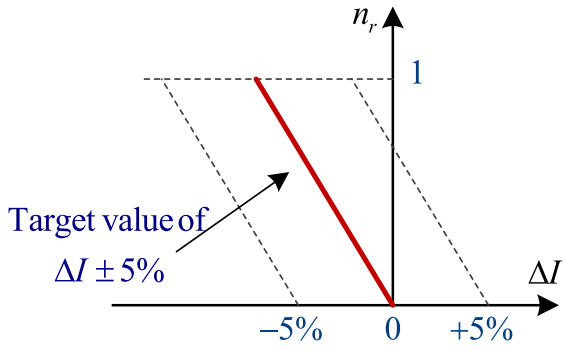

Fig. 1. The target range of the normalized axial offset [10].

2.2. Xenon oscillation and axial offset power-distribution

In a PWR, the axial xenon oscillation occurs over a long-time operation. This leads to an AO power-distribution. Failure to do so will result in a local power peaking issue. However, the radial power peaking factor is smoothed at the beginning of the fuel cycle (BOC). The AO is defined with the mean power deviation of the two core halves to the core power as Eq. (9) [10].

$$AO = \frac{P_2 - P_1}{P_2 + P_1} \tag{9}$$

The AO must be bound to the desired value, at the nominal power in the equilibrium state of the xenon and absence of the control rods [11]. The AO criterion is assessed with its normalized valued (Eq. (10)) in a $P - \Delta I$ coordinate

$$\Delta I = AO \times P \tag{10}$$

As shown in Fig. 1, the $P - \Delta I$ should be laid in the acceptable range (in this paper, 5%) during the reactor operation.

Also, a normalized axial xenon oscillation index (AXOI) is used to assess the core axial xenon oscillations of the core. This factor is defined by the normalized difference of the xenon concentration between two nodes to the total core as Eq. (11) [12].

$$AXOI = \frac{Xe_2 - Xe_1}{Xe_0} \tag{11}$$

2.3. Controller and optimization procedure

In this paper, the standard PID controller is considered, which is very popular in the NPPs. PID defined as Eq. (12) [13].

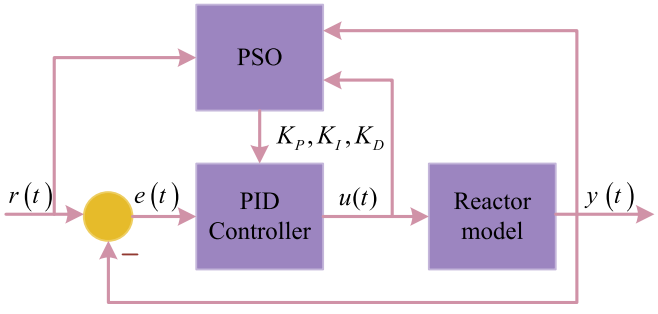

Fig. 2. Optimizing method. r: desired signal (desired power as set-point); y: output relative neutron density.

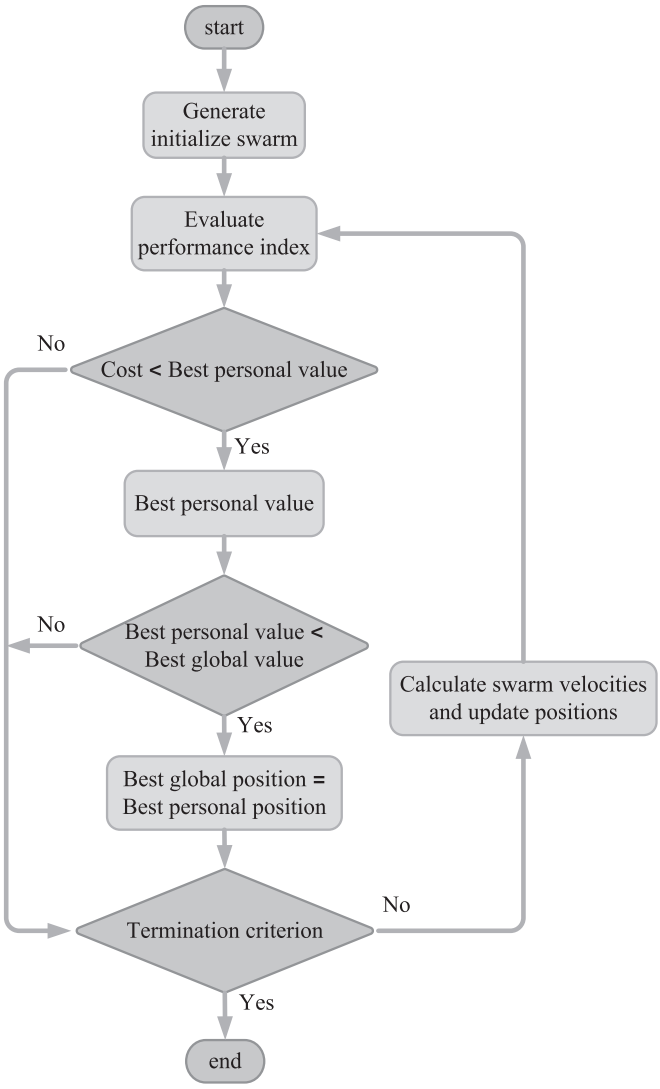

Fig. 3. PSO flowchart.

$$u(t) = K_P e(t) + K_I \int_0^t e(\tau)\mathrm{d}\tau + K_D \frac{\mathrm{d}}{\mathrm{d}t} e(t) \tag{12}$$

where $K_P, K_I, K_D \in \mathbb{R}$.

The PSO script code is added to the controlling system as Fig. 2. The PSO tunes the best gains of each PID related to each node, based on the desired signal (desired relative power/neutron density). The relative power of each node is set by the desired AO. The AO must remain constant during the load-following.

Table 1
The PSO parameters.

Parameters	Value
Members of each individual	$\begin{cases} K_{P1}, K_{I1}, K_{D1} \\ K_{P2}, K_{I2}, K_{D2} \end{cases}$
Maximum Iteration	100
Swarm size (N_{pop})	30
χ	0.7298
ω	0.7298
c_1	1.49609

Table 2
Analytical results of the optimizations and simulations.

Performance index		Region 1 (s)	Region 2 (s)	Region 3 (s)	Region 4 (s)
		150–250	250–750	750–850	850–1000
IAE	Euclidean norm	1.0411×10^{-4}	1.2488×10^{-4}	1.3868×10^{-4}	0.7269×10^{-4}
	Over/Under-shoot	2.5675×10^{-5}	8.0548×10^{-5}	7.0391×10^{-5}	2.7539×10^{-5}
	IAE	7.3616×10^{-5}	8.8300×10^{-5}	9.8050×10^{-5}	5.1399×10^{-5}
	ISE	0.3894×10^{-9}	2.2702×10^{-9}	1.7910×10^{-9}	0.3856×10^{-9}
	ITAE	0.012660329	0.022706374	0.075131504	0.044036373
	ITSE	0.5943×10^{-7}	5.6874×10^{-7}	13.446×10^{-7}	3.2830×10^{-7}
ISE	Euclidean norm	1.0419×10^{-8}	2.3329×10^{-8}	2.0340×10^{-8}	0.9358×10^{-8}
	Over/Under-shoot	2.5744×10^{-5}	5.2337×10^{-5}	4.9665×10^{-5}	2.6842×10^{-5}
	IAE	3.8844×10^{-4}	4.3045×10^{-4}	4.5080×10^{-4}	2.7085×10^{-4}
	ISE	3.3530×10^{-9}	7.9625×10^{-9}	6.8972×10^{-9}	3.0125×10^{-9}
	ITAE	0.068680059	0.113447765	0.347650939	0.23363066
	ITSE	0.5400×10^{-6}	2.0388×10^{-6}	5.2194×10^{-6}	2.5816×10^{-6}
ITAE	Euclidean norm	0.017904504	0.03205635	0.106171524	0.062336879
	Over/Under-shoot	2.5729×10^{-5}	19.328×10^{-5}	4.9195×10^{-5}	7.2495×10^{-5}
	IAE	7.3617×10^{-5}	8.8321×10^{-5}	9.7948×10^{-5}	5.1460×10^{-5}
	ISE	0.3901×10^{-9}	7.0792×10^{-9}	1.2784×10^{-9}	0.8366×10^{-9}
	ITAE	0.012660393	0.022667263	0.075074599	0.044071769
	ITSE	0.5954×10^{-7}	17.713×10^{-7}	9.6024×10^{-7}	7.1155×10^{-7}
ITSE	Euclidean norm	0.8404×10^{-7}	5.4964×10^{-7}	13.579×10^{-7}	4.2528×10^{-7}
	Over/Under-shoot	2.5675×10^{-5}	5.3382×10^{-5}	4.9194×10^{-5}	2.5342×10^{-5}
	IAE	7.3615×10^{-5}	8.8298×10^{-5}	9.7959×10^{-5}	5.1452×10^{-5}
	ISE	0.3893×10^{-9}	1.5494×10^{-9}	1.2783×10^{-9}	0.3532×10^{-9}
	ITAE	0.012660253	0.022729928	0.075082996	0.044087356
	ITSE	0.5942×10^{-7}	3.8863×10^{-7}	9.6014×10^{-7}	3.0071×10^{-7}

For each region of the power phase, all PID gains generated by the PSO algorithm are simulated in the dynamic model. The PSO scripts call the required outputs for evaluating its objective function at the end of the system dynamic model simulation. In the next iteration, new PID gains are generated by PSO, if the termination criterion of the algorithm loop is not reached.

2.4. Particle swarm optimization (PSO)

The PSO algorithm is a population-based stochastic optimization method designed by Eberhart and Kennedy [14]. The PSO algorithm is very similar to evolutionary computational techniques such as GA. The system starts by collecting random solutions and searching for optimization along with generation updates. Unlike GA, the PSO algorithm has no evolutionary operator such as crossover and mutation.

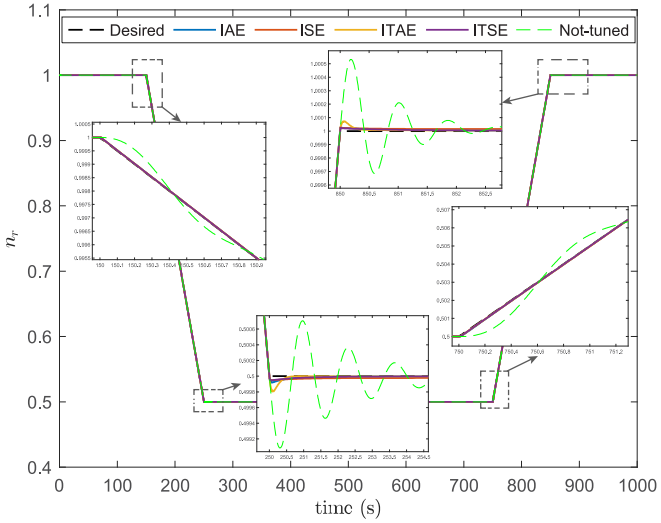

Fig. 4. Relative neutron density with tuned and not-tuned PID controllers.

2.4.1. Algorithm

The PSO algorithm starts with a group of random particles (the solution) and then searches for generations. In the first iterations, the agents are generated uniformly randomly, which are mapped to the desired real number gains for better system controllability based on the system-related experts (in this work, $0 < K_P < 100$, $0 < K_I < 100$, $0 < K_D < 10$), in the structure of the objective function. The value of each particle is measured with a cost function as a performance index. Each particle is updated with two best values in each iteration. The first is the best solution (fitness function) that has ever been achieved (the proportion value is also stored). This is called the "*pBest*" value. Another best cost is the value so far earned by individuals in the population. This is the best global value that is called "*gBest*". After finding the best values of the pBest and the gBest, the particle updates its velocity and position with Eqs. (13) and (14) in one-dimensional space. In this work, the velocity reflection method is used when the particle exceeds the border of the search space.

$$v_i^{t+1} = \omega v_i^t + c_1 \alpha \times \left(x_{i,pBest}^t - x_i^t\right) + c_2 \beta \times \left(x_{gBest}^t - x_i^t\right) \tag{13}$$

$$x_i^{t+1} = x_i^t + v_i^{t+1} \left(i = 1, 2, \ldots, N_{pop}\right) \tag{14}$$

where N_{pop}: number of particle swarm; t: generation indices; x_i: a position of the i-th particle; $x_{i,pBest}^t$: the best personal position of the i-th particle at the t-th generation; x_{gBest}^t: the best global position of all particles up to t-th generation; v_i: particle velocity of the i-th particle; ω: inertia weight; c_1, c_2: acceleration coefficients (learning factor); α, β: uniform random numbers.

Confidence factors are considered as $\omega = \phi$, $c_1 = \chi\phi_1$, $c_2 = \chi\phi_2$ [15], which ϕ and χ (construction factor), are based on the Clerc's method [16] as Eq. (15):

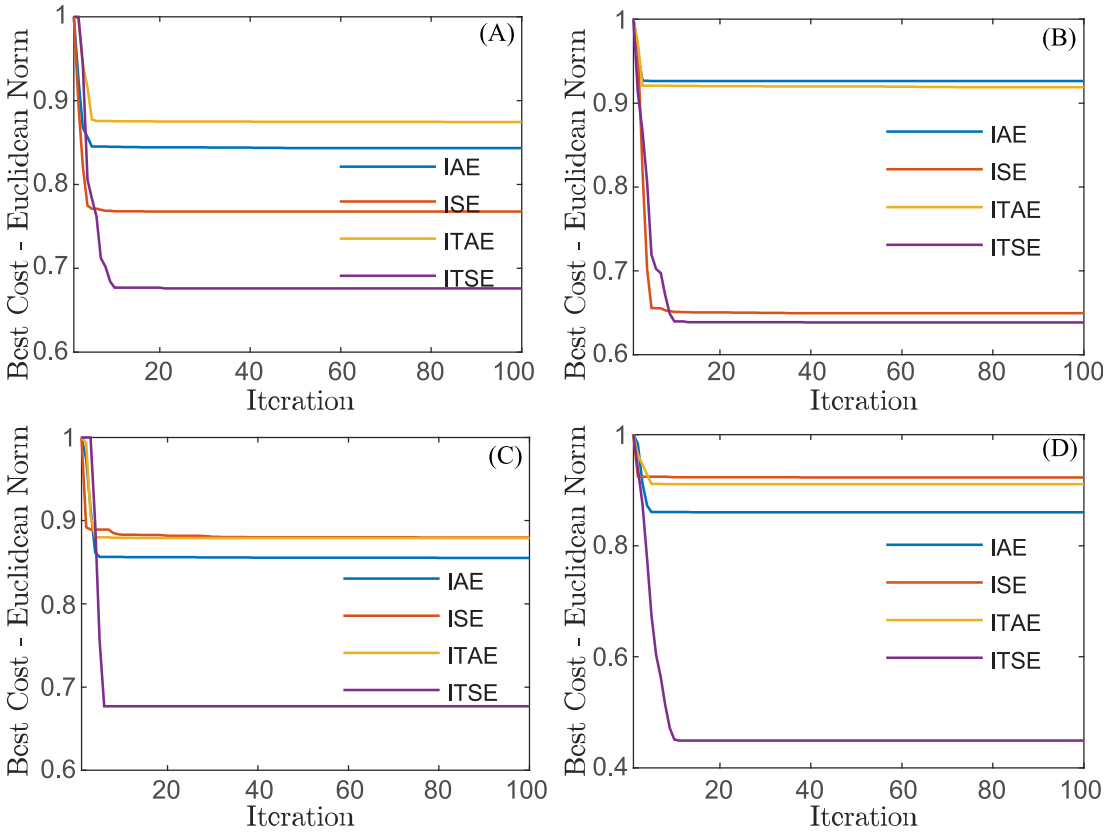

Fig. 5. Normalized Euclidean norm (cost) vs. the NFE at (A) region 1, (B) region 2, (C) region 3, and (D) region 4.

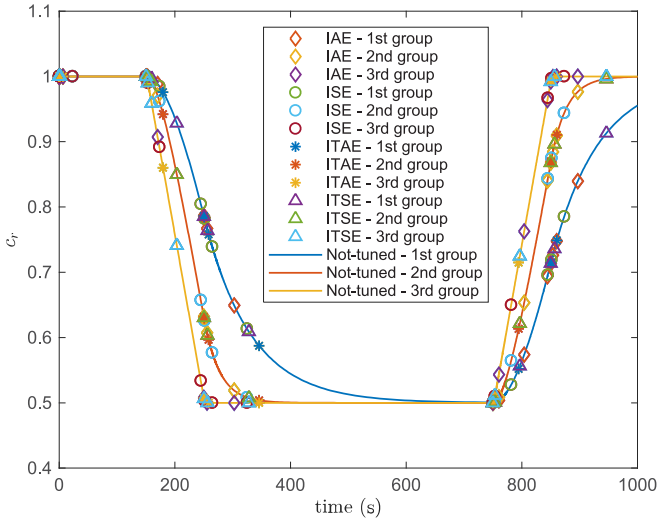

Fig. 6. Relative precursor density.

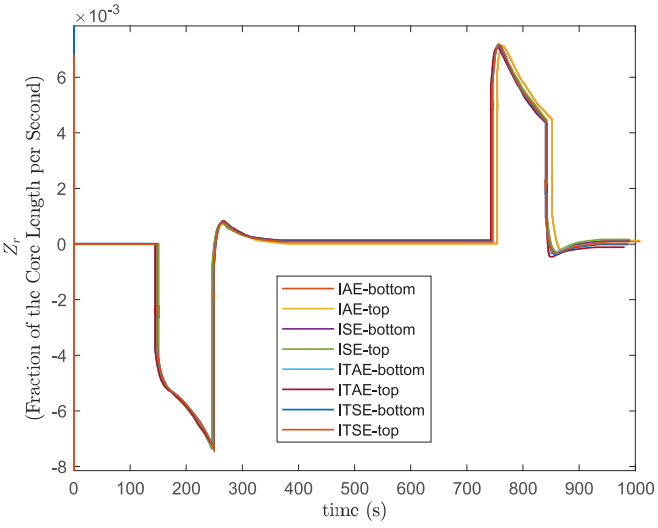

Fig. 7. Control rod speed (control signal) of the bottom/top core.

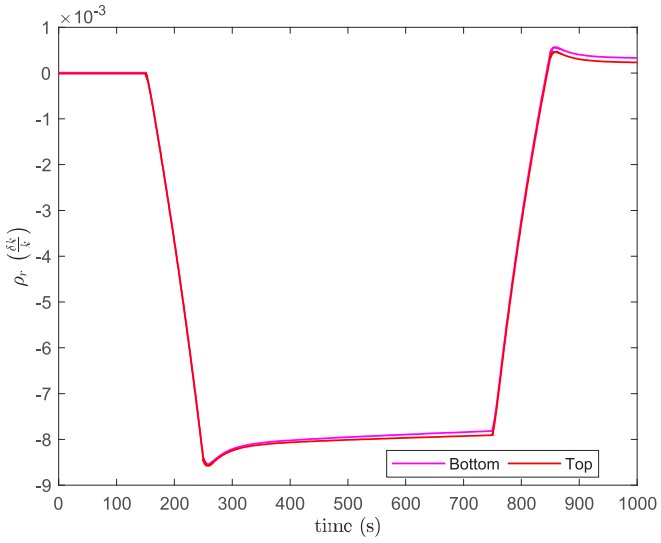

Fig. 8. Reactivity of the bottom/top control rod.

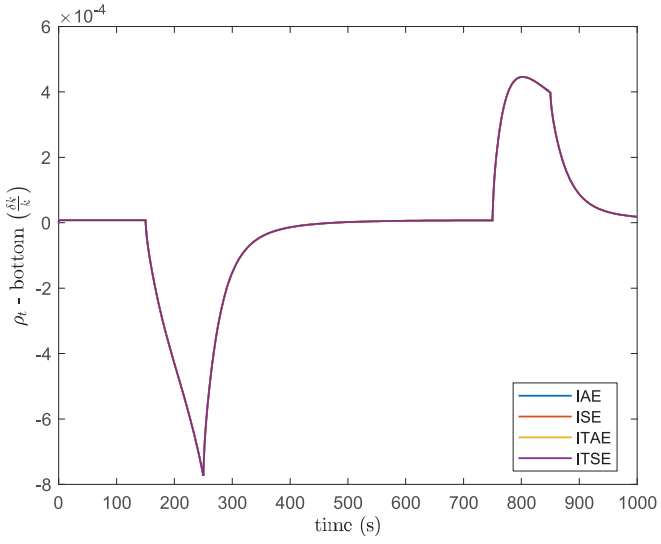

Fig. 9. Total reactivity of the bottom core.

$$\begin{cases} \forall\ \phi_1, \phi_2 > 0 : \phi \triangleq \phi_1 + \phi_2 > 4 \\ \chi = \dfrac{2}{\phi - 2 + \sqrt{\phi^2 - 4\phi}} \end{cases} \tag{15}$$

In this method, $\phi_1 = \phi_2 = 2.05$, and $\chi \approx 0.7298$.

The PSO flowchart is similar to Fig. 3. The iterations terminate after a certain number, based on try–and–error of the best cost convergence. Also, the used PSO parameters of this paper are based on Table 1.

2.4.2. Objective function definition

The particles are evaluated by a cost function as a performance index. IAE, ISE, ITAE, and ITSE objective functions are considered because of their good performance for PID as Eqs. 16–19, respectively.

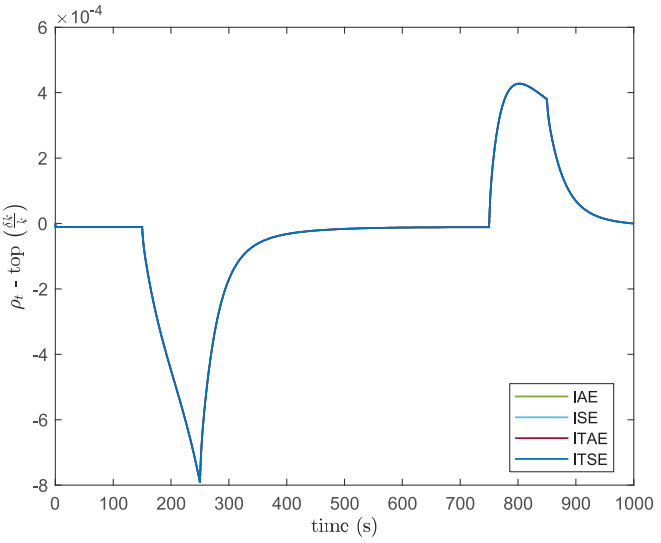

Fig. 10. Total reactivity of the top core.

$$IAE = \int_0^\infty |e(t)| \mathrm{d}t \tag{16}$$

$$ISE = \int_0^\infty e^2(t) \mathrm{d}t \tag{17}$$

$$ITAE = \int_0^\infty t|e(t)| \mathrm{d}t \tag{18}$$

$$ITSE = \int_0^\infty te^2(t) \mathrm{d}t \tag{19}$$

In the two-point kinetics model, two PIDs are optimized simultaneously. Distinct cost functions are defined for each node:

$$F_j = (\textit{desired performance index})_j \tag{20}$$

where F_j: cost function associated with each node.

Minimizing the cost function of one node may increase the cost of another node. Therefore, the Euclidean norm may be used as a Pareto front to maintain the balance between them [17]. On the Pareto front of this work, the minimum distance to the optimal response is considered. In this study, the ideal answer is zero. Hence, the main cost function (F) is defined in the Euclidean norm of the two cost functions as Eq. (21).

$$F = \sqrt{F_1^2 + F_2^2} \tag{21}$$

3. Results and discussion

The MATLAB/SIMULINK environment has been used to simulate the reactor dynamics model and the tuned PID. A short-time transient as the 100%→50%→100% power demand with the ∓30% /min ramp is considered for the controlling system and PSO

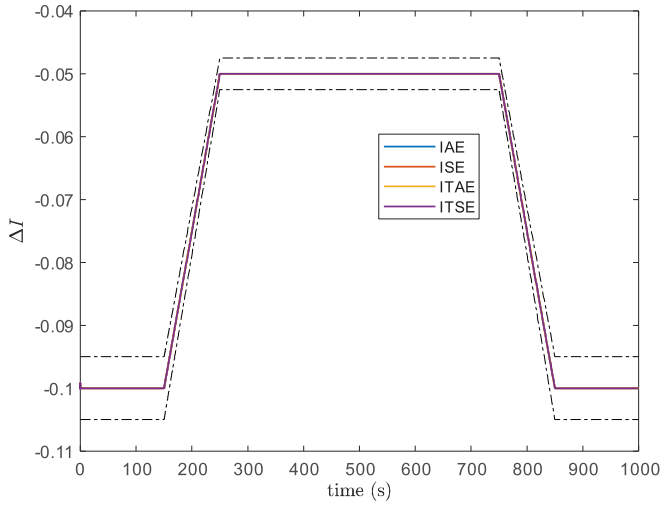

Fig. 11. Normalized AO (ΔI) of the core.

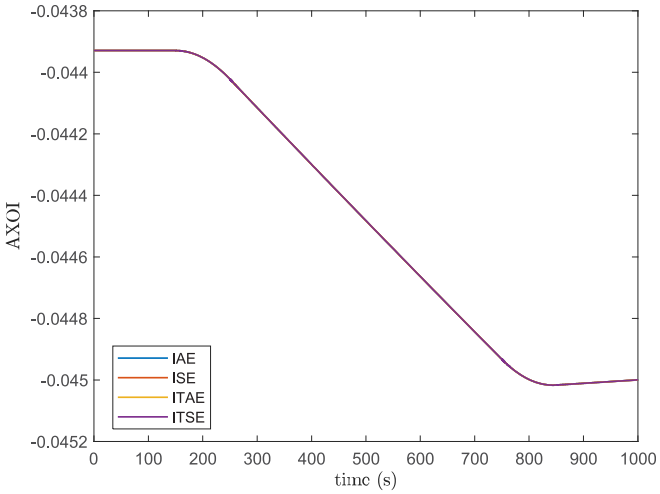

Fig. 13. Core AXOI.

optimization. The changing level is divided into four regions. Each region is controlled by a distinct PID, which is tuned by PSO. Table 2 illustrates the analytical result for each scenario of the performance indexes used in optimization. The Euclidean norm of the two nodes and over/under-shoot, IAE, ISE, ITAE, and ITSE results of the core are shown for each performance index method.

Fig. 4 shows the simulation results in the tuned and not-tuned (empirically tuned) controlling system.

Fig. 5 shows the normalized Euclidean norms (costs) over the NFE. It is generally shown that square error performance indexes have a lower cost value but delay convergence. Whereas the absolute error performance indexes have higher cost value, but faster convergence.

The relative precursor densities are shown in Fig. 6. Their behavior is proportional to the changes in power levels (Fig. 4).

Fig. 7 illustrates the bottom and top control rods speed (the control signal), which are important in applying to hardware drivers. It is observed that their oscillation range is limited by the length of the control rod without excess control requirement, in all performance indexes.

The induced reactivity of the control rods movement leads the core power to the desired value. The behaviors of two half control rods shown in Fig. 8 are smoothed considering their worth. It is observed the pattern of changes in the power level.

The small difference in power changes of the two nodes due to the low AO (−10% in this work), as well as the same behavior in power change, leads to similarity and proximity changes in the reactivities.

Figs. 9 and 10 are shown the total reactivity of the bottom and top core, respectively. In steady-states, i.e. regions 2 and 3, the total reactivities are limited to zero due to the reactivity feedbacks, based on all performance indexes.

Figs. 11 and 12 show ΔI over time and n_r over ΔI, respectively. It is shown, ΔI is bound into −10% n_r (1 ±5%) range.

Also, AXOI must be limited in an acceptable range. Fig. 13 illustrated this matter.

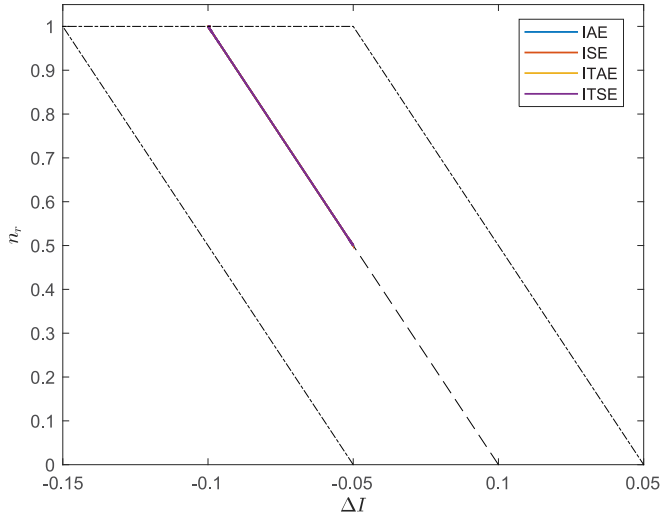

Fig. 12. Relative neutron density vs. the ΔI.

4. Conclusion

In this paper, the two-point kinetics model of a typical PWR nuclear reactor was considered for load-following issue by using a tuned standard PID. PID gains optimization was performed by the PSO algorithm. Conventional IAE, ISE, ITAE, and ITSE objective functions were assessed as performance indexes for PID gains optimization. It was shown that ITAE and ITSE have less over/under-shoot than IAE and ISE, especially in steady-state regions. Also, it was generally shown that square error performance indexes (ISE and ITSE) have lower cost value with delay in the convergence. Whereas the absolute error performance indexes (IAE and ITAE) have higher cost value with faster convergence. Eventually, by using all performance indexes in the PSO optimization algorithm, the results of the controlling system have good performance, fast control response, and accuracy than approximate and empirical tuning methods.

Declaration of competing interest

The authors declare that they have no known competing financial interests or personal relationships that could have appeared to influence the work reported in this paper.

References

[1] J.P. Câmara Augusto, A. Dos Santos Nicolau, R. Schirru, PSO with dynamic topology and random keys method applied to nuclear reactor reload, Prog.

Nucl. Energy 83 (2015) 191–196.
[2] P. Wang, J. Wan, R. Luo, F. Zhao, X. Wei, Control parameter optimization for AP1000 reactor using Particle Swarm Optimization, Ann. Nucl. Energy 87 (2015) 687–695.
[3] T.Y. Lin, J.T. Yeh, W.S. Kuo, Using particle swarm optimization algorithm to search for a power ascension path of boiling water reactors, Ann. Nucl. Energy 102 (2017) 37–46.
[4] A. Ahmad, S. ul I. Ahmad, Optimization of fuel loading pattern for a material test reactor using swarm intelligence, Prog. Nucl. Energy 103 (2018) 45–50.
[5] H. Wang, M. jun Peng, J. Wesley Hines, G. yang Zheng, Y. kuo Liu, B.R. Upadhyaya, A hybrid fault diagnosis methodology with support vector machine and improved particle swarm optimization for nuclear power plants, ISA Trans. 95 (2019) 358–371.
[6] W. Zeng, W. Zhu, T. Hui, L. Chen, J. Xie, T. Yu, An IMC-PID controller with Particle Swarm Optimization algorithm for MSBR core power control, Nucl. Eng. Des. 360 (2020), https://doi.org/10.1016/j.nucengdes.2020.110513.
[7] S.M.H. Mousakazemi, Computational effort comparison of genetic algorithm and particle swarm optimization algorithms for the proportional–integral–derivative controller tuning of a pressurized water nuclear reactor, Ann. Nucl. Energy 136 (2020) 107019.
[8] D.L. Hetrick, Dynamics of Nuclear Reactors, American Nuclear Society, 1993.
[9] P.F. Wang, Y. Liu, B.T. Jiang, J.S. Wan, F.Y. Zhao, Nodal dynamics modeling of AP1000 reactor for control system design and simulation, Ann. Nucl. Energy 62 (2013) 208–223.
[10] P.J. Sipush, R.A. Kerr, A.P. Ginsberg, Load follow demonstrations employing constant axial offset power distribution control procedures, Nucl. Technol. 31 (1976) 12–31.
[11] C.E. Meyer, C.L. Bennett, D.J. Hill, K.J. Dzikowski, Improved load follow strategy for return-to-power capability, Nucl. Technol. 41 (1978) 27–35.
[12] H. Eliasi, M.B. Menhaj, H. Davilu, Robust nonlinear model predictive control for nuclear power plants in load following operations with bounded xenon oscillations, Nucl. Eng. Des. 241 (2011) 533–543.
[13] K.J. Astrom, T. HÄgglund, Advanced PID control, ISA-The Instrumentation, Systems and Automation Society, 2006, https://doi.org/10.1109/MCS.2006.1580160.
[14] R. Eberhart, J. Kennedy, New optimizer using particle swarm theory, in: Proc. Int. Symp. Micro Mach. Hum. Sci., IEEE, 1995, pp. 39–43.
[15] R. Poli, J. Kennedy, T. Blackwell, Particle swarm optimization, Swarm Intell 1 (2007) 33–57.
[16] M. Clerc, J. Kennedy, The particle swarm-explosion, stability, and convergence in a multidimensional complex space, IEEE Trans. Evol. Comput. 6 (2002) 58–73.
[17] P. Ngatchou, A. Zarei, A. El-Sharkawi, Pareto multi objective optimization, in: Proc. 13th Int. Conf. on, Intell. Syst. Appl. To Power Syst., IEEE, 2005, pp. 84–91.